HHS Public Access

Author manuscript

*Immunity*. Author manuscript; available in PMC 2018 September 19.

Published in final edited form as:

*Immunity*. 2017 September 19; 47(3): 524–537.e3. doi:10.1016/j.immuni.2017.08.006.

# Glycans function as anchors for antibodies and help drive HIV broadly neutralizing antibody development

**Raiees Andrabi**[1,2,3,#], **Ching-Yao Su**[1,2,3,#], **Chi-Hui Liang**[1,2,3], **Sachin S. Shivatare**[4], **Bryan Briney**[1,2,3], **James E. Voss**[1,2,3], **Salar Khan Nawazi**[1,2], **Chung-Yi Wu**[4], **Chi-Huey Wong**[4], and **Dennis R. Burton**[1,2,3,5,6,*]

[1]Department of Immunology and Microbiology, The Scripps Research Institute, La Jolla, CA 92037, USA

[2]International AIDS Vaccine Initiative, Neutralizing Antibody Center, The Scripps Research Institute, La Jolla, CA 92037, USA

[3]Center for HIV/AIDS Vaccine Immunology and Immunogen Discovery, The Scripps Research Institute, La Jolla, CA 92037, USA

[4]Genomics Research Center, Academia Sinica, Nankang, Taipei 115, Taiwan

[5]Ragon Institute of Massachusetts General Hospital, Massachusetts Institute of Technology, and Harvard, Cambridge, MA 02114, USA

## Summary

Apex broadly neutralizing HIV antibodies (bnAbs) recognize glycans and protein surface close to the 3-fold axis of the envelope (Env) trimer and are among the most potent and broad Abs described. The evolution of apex bnAbs from one donor (CAP256) has been studied in detail and many Abs at different stages of maturation have been described. Using diverse engineering tools, we investigated the involvement of glycan recognition in the development of the CAP256.VRC26 Ab lineage. We found that sialic acid-bearing glycans were recognized by germline-encoded and somatically mutated residues on the Ab heavy chain. This recognition provided an “anchor” for the Abs as the core protein epitope varies, prevented complete neutralization escape, and eventually led to broadening of the response. These findings illustrate how glycan-specific maturation enables a human Ab to cope with pathogen escape mechanisms and will aid in optimization of immunization strategies to induce V2 apex bnAb responses.

## eTOC Blurb

[*]Correspondence: burton@scripps.edu.
[#]These authors contributed equally
[6]Lead contact



**AUTHOR CONTRIBUITIONS**

R.A. designed the experiments. R.A., C.Y.S, C.H.L., S.S.S., B.B., J.E.V., S.K.N. performed the experiments. C.Y.W., and C.H.W. contributed critical reagents. R.A. and D.R.B. analyzed the data and wrote the paper.

Understanding the molecular basis for the development of HIV Env-specific bnAbs is key for vaccine design. Andrabi et al. find that CAP256 V2 apex lineage Abs affinity mature with sialic acid containing complex-type glycans on HIV envelope trimer. This glycan recognition enables the development into bnAbs by resisting virus escape.

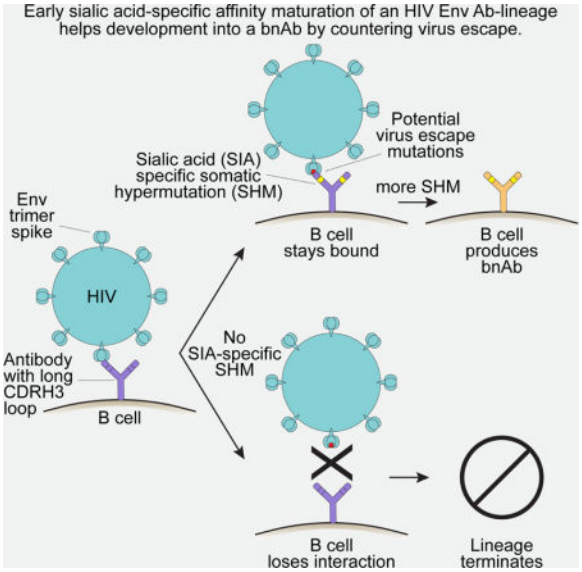


## Introduction

A promising track for HIV vaccine design is to take lessons from broadly neutralizing antibodies (bnAbs) and their interaction with Envelope trimer (Env) to craft potential immunogens in an approach described as “Reverse Vaccinology 2.0” (Burton, 2002; Rappuoli et al., 2016). It has become apparent that multiple immunogens will likely be required to guide the antibody response from their unmutated ancestors to bnAbs (Briney et al., 2016b; Dosenovic et al., 2015; Escolano et al., 2016; Jardine et al., 2015; Tian et al., 2016), including immunogens to trigger unmutated precursor B cells, to shepherd them along favorable pathways and to maximize their interaction with a broad spectrum of native Env molecules (Andrabi et al., 2015; Bhiman et al., 2015; Dimitrov, 2010; Doria-Rose et al., 2014; Gorman et al., 2016; Jardine et al., 2013; Liao et al., 2013; McGuire et al., 2016; Steichen et al., 2016; Xiao et al., 2009). One of the targets of bnAbs that has attracted a great deal of attention is the V2 apex region of Env (Andrabi et al., 2015; Bhiman et al., 2015; Doria-Rose et al., 2014; Sok et al., 2014; Walker et al., 2011; Walker et al., 2009). bnAbs to this region are induced in a substantial proportion of the individuals who make such Abs (Georgiev et al., 2013; Landais et al., 2016; Walker et al., 2010) and the V2 apex response tends to appear earlier in natural HIV infection than other bnAb responses (Doria-Rose et al., 2014; Wibmer et al., 2013), both factors that favor it as a vaccine target.

The V2 apex represents a complex antigenic region. Broadly speaking, a lysine-rich set of residues on V2 come together in space around the 3-fold axis at the “top” of the spike to constitute a basic region that is recognized by acidic residues (aspartate and sulfated tyrosines) at the tip of a long HCDR3 (heavy chain complementarity-determining region 3

of the heavy chain) of the bnAb. In order to access the basic region, the HCDR3, and to some extent the other CDRs, of the bnAb must penetrate the glycan shield of Env and particularly interact with and/or accommodate a conserved glycan at N160 and, to a lesser extent, a second nearby glycan at N156 or rarely N173 (Amin et al., 2013; Gorman et al., 2016; Lee et al., 2017; McLellan et al., 2011; Pancera et al., 2013; Walker et al., 2009). Detailed studies have combined structure, nuclear magnetic resonance (NMR) and mutagenesis analysis to characterize glycan recognition by the V2 apex bnAbs PG9 and PG16 (McLellan et al., 2011; Pancera et al., 2013). These studies identified PG9 and PG16 as interacting with a $Man_5GlcNAc_2$ structure at N160 and a sialic acid containing hybrid-type glycan at N173 or N156. The studies employed V1V2 loops on scaffolds rather than native Env and this remains a caveat to this analysis. Particular focus was placed on a terminal sialic acid on the glycan at N173 or N156 interacting with a tripeptide (RSH) motif in the light chain of PG16.

The molecular information provided by these studies is extremely valuable but more insight is needed prior to embarking upon a systematic multistage vaccine effort to target the V2 apex region. One approach is to compare different V2 apex bnAbs and identify common features that could be important in considering immunogen design. This approach has been valuable in identifying potential V2 apex bnAb precursor-targeting immunogens (Andrabi et al., 2015; Gorman et al., 2016; Sanders et al., 2015) that are currently under study. Four prototype V2 apex bnAb lineages have been described and two of them, PG9 and CAP256-VRC26, are derived from variable heavy chain (VH) gene segments that show 99% sequence identity and use the same D-gene that provides critical anionic residues for protein epitope recognition (Andrabi et al., 2015; Bonsignori et al., 2011; Doria-Rose et al., 2014; Walker et al., 2011; Walker et al., 2009). A second approach is to investigate the co-evolution of bnAb and virus during natural infection to identify critical stages in the maturation of the response and attempt to extract information that can aid in immunogen design (Doria-Rose et al., 2014; Liao et al., 2013; MacLeod et al., 2016). The CAP256 lineage (referred to as CAP256.01-33) has been extensively studied and first appeared following superinfection of the donor. This lineage has a particularly long HCDR3, which is 35 amino acids (Kabat numbering convention) in the Unmutated Common Ancestor (UCA) and increases by insertions to 37 amino acids in the most potent mature bnAbs (Doria-Rose et al., 2016; Doria-Rose et al., 2014). One detailed study of co-evolution in the CAP256 lineage showed different fates for Abs originating in the UCA. One track led to “dead-end” Abs that did not evolve as they could not respond to viral diversity. A second track continued to evolve resulting in highly somatically mutated Abs, some that were able to neutralize many viral variants as well as “off-track” Abs that were limited in their neutralization breadth (Bhiman et al., 2015).

Here, we sought to take advantage of the availability of Abs from the CAP256 lineage to study the role of glycan interactions in the evolution of the lineage. We compared a number of features of the interactions of CAP256 Abs with glycans and investigated the role of glycan recognition in resisting neutralization escape. We concluded that recognition of sialic acid-bearing glycans was critical in the evolution of CAP256 family antibodies, depended upon germline-encoded and somatically mutated residues in CDRH2, and acquisition of

these somatic mutations early in Ab maturation could help anchor Abs to their epitope even in the face of mutations in the core protein part of the epitope.

## Results

### CAP256 lineage Abs evolve in terms of glycan recognition during affinity maturation with possible contribution from terminal sialic acids

The four V2 apex bnAb prototype lineages, PG9, CH01, PGT145 and CAP256.09 typically depend on glycans at positions N160 and N156, or less often N173 (McLellan et al., 2011; Pancera et al., 2013; Walker et al., 2009), for neutralization and binding to the Env trimer. The N173 glycan site is relatively close to the N156 site and it appears that the N173 glycan can act to replace the N156 glycan in the context of certain isolates in the binding of V2 apex bnAbs (McLellan et al., 2011; Pancera et al., 2013). The first three Ab prototypes show an absolute dependence on the N160 glycan site for neutralization whereas the dependence is variable with respect to glycan N156 or N173. In contrast, the neutralizing activity of the CAP256.09 Ab prototype is partially dependent on both N156 or N173 and N160 glycans in an isolate and context-dependent manner (Doria-Rose et al., 2016; Doria-Rose et al., 2014).

To assess the dependency of CAP256 lineage Abs during maturation on Env glycans and glycan character in detail, we employed three approaches. We carried out our studies in the context of the CRF250 isolate trimer as this isolate binds to inferred-unmutated ancestor versions of multiple V2 apex bnAb prototypes and represents a potential B cell precursor targeting immunogen (Andrabi et al., 2015).

First, we generated CRF250 Env virus variants that lacked glycans at positions N156 and N160 and investigated neutralization by CAP256 lineage members (Figure 1A–B and S1). The wild-type (WT) CRF250 virus grown in 293T cells was neutralized by all CAP256 Ab lineage members, with the exception of Ab CAP256.20. This pattern was similar to that seen for the CAP256 superinfecting virus (CAP256.SU), highlighting the antigenic resemblance of CRF250 Env and the CAP256.SU Env, which, or a close descendant thereof, is believed to have led to initiation of the CAP256 Ab lineage (Figure 1B and S1) (Bhiman et al., 2015; Doria-Rose et al., 2016). Both N156 and N160 glycan eliminated variants were less well neutralized by CAP256 bnAbs, the effect being more prominent with N156 glycan elimination (N156A; 882-fold drop) than N160 glycan removal (N160A; 80-fold drop in average IC50 compared to the WT CRF250 virus (Figure 1B and S1). Effects were seen throughout the lineage although the most potent neutralizing Abs to CRF250, CAP256.03 and .25, tolerated the loss of the N160 glycan very well (Figure S1).

As a second approach to glycan dependence of Ab binding, we modified the glycan composition on the CRF250 Env trimer by growing virus in the presence of the glycosidase inhibitors, kifunensine (ER α - mannosidase I inhibitor) and swainsonine (Golgi α-mannosidase II inhibitor) and in 293S cells, which lack an N-acetyl glucosaminyl transferase enzyme. Kifunensine-treated cells were expected to yield viruses with mostly high mannose ($Man_{8–9}GlcNAc_2$) glycans; swainsonine-treated cells to yield viruses with high mannose or hybrid-type glycans with a $Man_5GlcNAc_2$ glycan core and a branch that may potentially terminate in a sialic acid (Doores and Burton, 2010; Pancera et al., 2013); and 293S cell-

grown viruses to have $Man_{5–9}GlcNAc_2$ glycans without any hybrid or complex-type glycan character. Neutralization sensitivity was substantially reduced by kifunensine treatment (a 58-fold increase in average IC50 titers) implying that binding of CAP256 Abs was disfavored by high-mannose only glycans ($Man_{8–9}GlcNAc_2$) at one or both of the N156 and N160 positions. In contrast, neutralization sensitivity was increased by swainsonine treatment as compared to the WT CRF250 virus, suggesting a preference for hybrid glycans at either position. The 293S cell-treated virus overall showed a decrease in neutralization compared to 293T-WT virus (a 28-fold drop in average IC50 titers); however, this drop in IC50 titers appeared to be mainly contributed by the later Ab lineage members (Figure 1B and S1). This latter observation was again consistent with an apparent preference for hybrid glycans, especially as the lineage progresses.

To give insight into the glycans recognized at the N156 and N160 positions on by the CAP256 bnAbs, we combined the CRF250 Env glycan eliminations at N156 and N160 with glycan modifying reagents to produce homogenous virus glycovariants. One caveat of this analysis was that the modifications could affect glycan processing that may, in turn, influence protein folding in the V2 apex region and thus Ab accessibility to the region. Nevertheless, we considered it useful to study the effects of modifications on one glycan in the absence of the other. We observed an increase in neutralization sensitivity to the CAP256 bnAbs, when the CRF250 N156A virus was produced in the presence of kifunensine while swainsonine treatment had little to no effect (Figure S1A and S1D). These results suggest that the CAP256 bnAbs prefer high mannose glycans ($Man_{8–9}GlcNAc_2$) at the N160 glycan position but that the native sugar at this position seems to include some proportion of hybrid or complex-type. In contrast, the CRF250 N160A virus with kifunensine had an overall opposite effect on neutralization sensitivity (Figure S1A and S1E), suggesting that a smaller high mannose or one with hybrid or complex glycan character may be preferred at the N156 position. Again, the above caveat should be noted.

As a third approach to glycan dependence of Ab binding, we tested CAP256 mAbs binding to a variety of human glycans on glycan microarrays. This approach revealed a strong binding of the more mature CAP256 Ab lineage members to bi, tri and tetra antennary glycans with α2–6 linked sialic acid residue as a terminal sugar (Figure 1C and S2A–B). As for the CAP256 Ab members here, V3-glycan PGT121 bnAb lineage members have been previously shown to bind complex-type glycans terminating with α2–6 linked sialic acid residues (Mouquet et al., 2012). The early CAP256 Ab members showed no detectable interaction-this does not mean that there is no contact of these early Abs with sialic acid. Indeed, data presented in the next section suggested there is contact. However, such contact must presumably involve a weaker interaction. A failure to detect glycan binding on arrays despite interaction being shown between Ab and glycan on a native Env structure has been previously described (Julien et al., 2013).

To specifically probe the importance of sialic acid recognition by the CAP256 Ab lineage on the native Env trimer, we investigated the effects of sialidase treatment of CRF250 SOSIP trimer on the binding of CAP256 Abs by Bio-Layer Interferometry (BLI) or Octet. We treated the CRF250 SOSIP.664 trimer with α2,3- or α2,6-sialidases alone or with a cocktail of α2,3- 2,6- 2,8- and 2,9-sialidases to remove terminal sialic acid specific glycosidic

linkages. We assessed the binding of the CAP256 Ab lineage members to the WT CRF250 trimer and its three desialylated forms. Octet revealed that the binding of CAP256 Abs to α2,3-sialidase-treated CRF250 trimer remained mostly uniform throughout the lineage and only a small fraction of Abs showed small changes in binding to the α2,3-desialylated protein as compared to the WT trimer (Figure 1D and S2C). However, for α2,6-sialidase-treated trimer, a number of later more mature Abs showed a trend for somewhat weaker binding as compared to WT trimer, consistent with array data (Figure 1D and S2C). The effect was most pronounced for the CAP256.21 mAb. In contrast to the later Abs, the earlier Abs did not show any noticeable α2,6-sialidase effects in line with their lack of binding to arrays expressing α2,6-sialic acid.

Overall, the findings suggest that the CAP256 lineage Abs have evolved in terms of glycan recognition during affinity maturation and there is an indication that binding of terminal sialic acids contributes.

## Critical CAP256 antibody residues for sialic acid recognition are located in the CDRH2

To better understand how sialic acid recognition evolves during CAP256 Ab lineage development, we sought to identify the most critical CAP256 Ab residues for glycan recognition and investigate how these residues were maintained or evolved during maturation of the response. We focused on the heavy chain (HC) of the CAP256 Abs since this chain dominates the activity of these Abs. Analysis of the HC sequences revealed 9 amino acid positions, including 4 positions in CDRH2 and 5 positions in CDRH3, that could potentially differentiate glycan-reactive Ab sub-lineage members from non-reactive ones (Figure S3A). We chose CAP256.09 as a prototype Ab from the glycan-reactive Ab sub-lineage and generated single amino acid substitutions at the above 9 positions in the HC. The WT Ab and its variants were tested for neutralizing activity against CRF250 virus and for binding to soluble CRF250 and BG505 SOSIP.664 trimers by Octet (Figure S3B). With the exception of K100S-A Ab variant, whose neutralizing activity with CRF250 virus was slightly enhanced, the neutralizing and binding activities of all the CAP256.09 Ab variants was reduced substantially as compared to the WT Ab indicating that the substituted residues contribute to neutralization and trimer binding.

To specifically identify residues in HC most critical for glycan recognition, we first assessed the binding of CAP256.09 WT Ab and nine variants to glycans on a microarray. The WT Ab reacted strongly to α2,6 linked sialic acid residue-containing glycans while the CDRH2 variants (D53A, K57A, H59A and W64A) Ab variants, in addition to a single CDRH3 variant (A100X-G), lost binding to the these glycans (Figure 2A). A similar glycan binding pattern was observed for a more potent CAP256 Ab lineage member, CAP256.25, and its corresponding CDRH2 Ab variants (Figure 2B), thus suggesting a role for these germline and somatically mutated residues in recognition of α2,6 linked sialic acid on glycans.

Previously, we showed that the VH-germline gene families of the CAP256 and PG9 or PG16 Ab lineages share amino acid sequence similarities (Andrabi et al., 2015). Analysis of the mature VH-gene of the CAP256 and PG9 Ab lineages revealed a common maturation pattern in the CDRH2 residues of the two lineages (Y59 to H and K64 to W) (Figure 2C). The data suggest this pattern may be associated with the critical nature of these residues for

glycan recognition. Indeed, functional analysis of the CDRH2 substitutions in the context of PG9 and PG16 bnAbs showed a similar dependence on the glycans as CAP256 Ab lineage members (Figure S3C–F). Examination of the crystal structure of PG9 and CAP256.09 bnAb prototypes shows that the four residues discussed above are close to each other and form a cage-like structure with K57 and H59 residues at the center (Figure 2D).

Overall therefore we observed two genetically related Ab lineages following a conserved affinity maturation pattern that helps them to recognize sialic acid-containing glycans on HIV Env trimer.

## Both germline and somatically mutated CAP256 CDRH2 residues contribute to Env binding and neutralization but the latter are most important

We next sought to assess how the CDRH2 germline and somatically mutated residues identified above contributed to V2 apex bnAb binding to Env and neutralization, in particular in the context of the critical glycans at N160 and N156. Previously, a number of structural and analytical studies have argued the presence of both high-mannose and complex-type glycans at glycan positions N160 and N156 (or occasionally N173) on diverse isolates (Amin et al., 2013; Behrens et al., 2016; Gristick et al., 2016; McLellan et al., 2011; Pancera et al., 2013). Further, structural studies have shown that PG9 and PG16 Abs make contact with N160 and N156 or N173 glycans on Env V2 scaffolds through both germline and somatically mutated residues (McLellan et al., 2011; Pancera et al., 2013).

To investigate, we generated a series of N156 or N173 and N160 glycan eliminated variants on a panel of diverse Env backgrounds. We tested these viruses and the glycan mutants in neutralization against 2 WT V2 apex bnAbs, PG16 and CAP256.25 and their corresponding CDRH2 variants (Figure 3A). For PG16 Ab and its Ab variants, neutralization was invariably completely eliminated on all N160 glycan removed Env mutants. This feature rendered it impossible to separate effects of the CDRH2 substitutions on N160 and N156 or N173 glycan interaction. However, CAP256 Ab lineage member retained some activity in many cases in N160 and N156 or N173 eliminated mutations allowing the corresponding glycan deficient viruses to be used to explore the behavior of the glycans individually as described earlier, although now in the context of the contribution of the CDRH2 substitutions to binding to each glycan. Again, we note the caveat that the loss of one glycan may impact the processing of the other.

Focusing on WT CAP256 Ab lineage member, CAP256.25, whose neutralizing activity was previously shown to be less affected by eliminating glycans (Doria-Rose et al., 2016), we noted a dependence of neutralization on the glycans N156 and N160 in an isolate and context-specific manner, the loss of neutralizing activity being more common for the N160 glycan elimination i.e. when N156 was the remaining glycan (Figure 3A). Considering next neutralization of the WT viruses by the two germline CDRH2 Ab variants (D53A and K57A), we showed limited reduction (up to 18-fold) in the neutralizing activities as compared to the WT CAP256.25 Ab. However, substitutions involving two of the CDRH2 somatic mutations (H59A and W64A), the WT virus neutralizing activities of the Ab variants were significantly reduced with the effect being generally more pronounced for the W64 residue substitution (>1000 fold IC50 change) (Figure 3A). Focusing then on the

CDRH2 variant Abs (D53A and K57A) neutralizing the N160A and N156A viruses, we observed a similar sensitivity pattern as that of the WT CAP256.25 Ab, suggesting the germline residues contribute in a limited way to neutralization through their interactions with the Env glycans. In contrast, the CDRH2 somatically mutated substituted Ab variants, particularly involving the H59A substitution, showed some very marked differences with N160 glycan eliminated viruses from WT CAP256.25 Ab. Figure 3A illustrates considerable decreases or even complete loss of neutralizing activity in some cases (Figure 3A). For example, Figure 3B shows that WT CAP256.25 Ab neutralizes two representative viruses, CAP45_G3 and Du156_12, and their N160A and N156A variants but the H59A variant Ab is far less effective against the N160A viruses. Far less dramatic effects are seen for the N156A virus implying that interaction of the CDRH2 somatic mutated residues with the N156 glycan (the remaining key glycan in the absence of N160) that is most important for the effects observed.

We also included in this analysis a CAP256 Ab lineage member, CAP256.12, that had accumulated somatic mutations comparable to the other CAP256 bnAb members, including the two glycan-specific CDRH2 somatic mutations, but failed to show broad-reactivity to the viruses (an “off-track Ab” in the nomenclature of Moore and colleagues (Bhiman et al., 2015)). The results revealed that the CAP256.12 Ab could only efficiently neutralize certain isolates when the glycan at position N160 was eliminated, suggesting that this Ab may have failed to accommodate or affinity mature with respect to the N160 glycan (Figure 3A).

Overall, the results demonstrate that both the germline and somatic mutated CDRH2 key heavy chain residues contribute to neutralization by CAP256.25 and PG16 but that somatically mutated residues are likely most important. Further, N156 may harbor the interacting sialic acids.

## N156 glycans may bear the terminal sialic acids that contact the key heavy chain residues on CAP256 and PG9 family antibodies

We wished to obtain further evidence for the glycan or glycans that bear the sialic acid targeted by CAP256 Abs. We incorporated substitutions on the CRF250 SOSIP backbone to individually eliminate each of the four V1V2 apex glycans, N135, N141, N156 and N160 in turn, reasoning that treatment with α2,6 sialidase and comparison to the effect on WT trimer might reveal which of the glycans was most likely to harbor the critical sialic acid(s) (Figure 4A). Due to the inability of PGT145 Ab to bind N160 glycan eliminated trimers (Andrabi et al., 2015), we chose 2G12 Ab to purify the WT CRF250 trimer and its single glycan variants prior to α2,6 sialidase treatment. Octet was used to investigate the binding of a selection of CAP256 mAbs to the glycovariants untreated or treated with α2,6 sialidase.

The effects of sialidase treatment were particularly marked for mAb CAP256.21. producing generally greatly reduced binding. The N156A variant showed lower binding overall and a lesser effect of sialidase treatment, implying that this Ab is dependent upon a sialic acid at N156. Of note, CAP256.21 Ab bound the N160A variant trimer with a higher affinity than even the WT CRF250 trimer, presumably involving an increased dependence on the N156 glycan in the absence of the N160 glycan (Figure 4B). However, upon α2,6 sialidase treatment, binding of CAP256.21 was dramatically lost, indicating that the sialic acid-

specific interaction of this Ab at least is mediated through the N156 glycan. The binding of CAP256.25 bnAb to WT CRF250 trimer and glycan modified variants showed reduced binding responses upon α2,6 sialidase treatment, except for the N156A variant, to which the relatively low binding response remained largely unchanged upon desialylation (Figure 4B and S4B). Overall, for WT, N135A and N141A CRF250 trimer variants, the effects of sialidase were modest for most Abs (Figure S4A–B). For the N160A variant, the effects of sialidase were somewhat greater (Figure S4A–B). Therefore, although the earlier data provides evidence as to the interaction of CAP256 Abs with sialic acid, the glycan elimination studies here suggest possible involvement of N156 but they do not unambiguously determine the glycan involved.

In earlier studies, structural analysis of the PG16 Ab with a V1V2 scaffold showed that the terminal sialic acid residue at glycan N173 makes one and two hydrogen bonds respectively with the CDRH2 germline-encoded residue K57 and the somatically mutated residue H59, in addition to three hydrogen bonds with PG16 Ab light chain residues (Figure 4C) (Pancera et al., 2013). Of note, however, the PG16 Ab showed an enrichment of only 2% of the total ZM109F V1V2 on scaffold that possessed the appropriate glycoforms, suggesting an inherent glycan heterogeneity at this site and a strong preference of PG16 to bind α2,6-linked sialic acid containing glycoforms. Recent studies using chromatography coupled mass spectrometry analysis of soluble Env proteins, suggested that the N156 glycan position is occupied largely by a high mannose glycan (Behrens et al., 2016; Panico et al., 2016). Another study (Cao et al., 2017) indicated that N156 is occupied either by high mannose or complex glycans for several soluble SOSIP.664 trimers, including the CRF250 trimer used in this study. Further studies are required to fully understand the compositions of the glycans in the V2 apex region on different isolates and expressed from different cell types. It should also be noted that only a sub-population of N156 or N173 glycan may be sialylated but this may be sufficient to drive sialic acid specific affinity maturation in two independent V2 apex bnAb lineages.

Altogether, these results are consistent with the importance of a sialic acid residue, possibly on the glycan N156 or N173 at the V2 apex site, in driving the affinity maturation of the CDRH2 residues, Y59 to H and K64 to W, in CAP256 and PG9 V2 apex bnAb prototypes.

## Improved sialic acid binding is associated with development of bnAbs; failure to mature such binding leads to non-bnAbs

To gain a better understanding of the importance of sialic acid recognition and the Ab mutations described above on bnAb development, we assessed the effects of sialidase treatment of CRF250 trimer on binding by the complete set of CAP256 Abs. We ranked the set of Abs according to the percentage change in octet binding (Figure 5A–B). The CAP256 Abs that displayed the most significant loss of binding (red color) upon removal of α2,6 linked sialic acid (CAP256.21, CAP256.30, CAP256.31, CAP256.12 and CAP256.13) had either the germline CDRH2 residue, D53, mutated to E or had both CDRH2 germline residues D53 and K57 mutated to A and Y respectively (Figure 5A–B). All 5 of these Abs became “off target” Abs suggesting that an “over-dependence” on sialic acid might be detrimental to the development of neutralization breadth. In contrast, CAP256 Ab members

that retained the germline residues Y59 and K64, or mutated at these positions to residues other than H at 59 and W at 64, generally showed enhanced binding to the α2,6 linked sialic acid-trimmed CRF250 trimer (Figure 5A–B (yellow in Figure 5B)). Thus, the unmutated ancestor version of CAP256 Abs may actually bind better to trimers lacking sialic acid.

In the middle part of Fig 5A (light red) are Abs that showed very modest changes upon removal of α2,6 linked sialic acid. These Abs typically have D53-K57-H59-W64 and show the greatest breadth of neutralization. For example, the broadest neutralizing Ab member, CAP256.25, exhibited very modest dependence on the α2,6 linked sialic acid. Thus, the data suggest that it may be vital for a developing bnAb to initiate sialic acid recognition but then keep a fine balance and not become over focused on sialic acid. Subsequently, this ability of the most mature CAP256 bnAb members to recognize broad diversity of features within the V2 apex epitope, including a reduced dependence on sialic acid bearing glycans, may increase their effectiveness against a wide range of viruses. The bnAbs may not only neutralize viruses with more varied protein epitopes but also tolerate glycoform heterogeneity at this site.

To further examine if the sialic acid specific affinity maturation of the glycan-specific CAP256 Ab sub-lineage was beneficial for the overall development of broad and potent Ab sub-lineage members, we analyzed Next-Generation Sequencing (NGS) data of B-cell transcripts from the CAP256 donor reported previously (Doria-Rose et al., 2016; Doria-Rose et al., 2014). The phylogenetic tree showed a strong bias towards the development of CAP256 Ab sub-lineage members that had accumulated sialic acid specific CDRH2 somatic mutations (Figure 5C).

Overall, these results suggest that affinity maturation in a subset of CAP256 Ab lineage members to improve sialic acid binding provides them a selective advantage in the progression toward a bnAb phenotype. Another subset of lineage members becomes over-dependent on sialic acid binding, loses some interaction flexibility and shows moderate neutralization breadth. A third subset fails to acquire the crucial mutations to effectively interact with sialic acid and shows little or no breadth of neutralization.

## Maturation of CAP256 antibodies to bind glycans counters viral escape occurring through protein sequence variation and promotes bnAb development

Glycan-specific maturation is advantageous for the overall development of the CAP256 Ab lineage. Next, we sought to examine if glycan recognition provided a means to counter virus escape. We generated virus mutants in CRF250 Env at positions R166 (R166 to K, T and S) and K169 (K169 to R, Q and E) to mimic the virus escape mutations that occur naturally in the CAP256 donor (Bhiman et al., 2015; Doria-Rose et al., 2014). We then tested these CRF250 virus mutants against the entire panel of CAP256 Abs by neutralization. Strikingly, only Abs with somatic mutations in the CDRH2 region (Y59H and K64W) associated with sialic acid binding tolerated the R166T escape mutation (Figure 6A–B and S5A). The same result was found for K169 escape mutations with the exception of CAP256.19 and CAP256.32, which tolerated K169Q escape mutations (Figure 6B and S5A). These observations suggest that the glycan-specific Ab mutations may provide a selection

advantage to the CAP256 sub-lineage members to cope with viral escape occurring via mutation of strand C residues during infection.

To further investigate, we tested the ability of CDRH2 residue substituted Ab variants on the background of CAP256.25, to neutralize apex bnAb putative escape variants of CRF250 (Figure 6C and S5B). As earlier, the CAP256.25 Ab Ala-substituted variants are less effective, by up to >1,000-fold, in terms of neutralization than WT Ab. However, the CDRH2 substitutions (H59A and W64A) eliminated neutralization of both R166K and K169Q CRF250 virus variants and reduced neutralization of the K169R virus mutant, under conditions for which the WT Ab is still neutralizing. These observations are consistent with the notion that the CDRH2 somatic mutations may help to counter neutralization escape via mutation in the V2 protein region.

Next, we investigated the binding of CAP256.25 WT Ab and variants to CRF250 WT Env trimers and escape variant Envs on the surface of 293T cells by flow cytometry. CAP256.25 WT Ab and variants bound strongly to CRF250 WT Env trimer. The WT Ab and variants exhibited significant binding to Env trimer from escape variants (R166 to T or S and K169E) that were not neutralized by the corresponding Abs (Figure 6D and S5C). The data suggest that the Env strand C residue mutations lead to the loss of neutralization at the Ab concentrations measured but trimer binding can still be detected (Figure 6D). However, the CAP256.25 CDRH2 somatic mutation substituted Ab variants completely lost binding to the surface expressed Env trimer variants R166T, R166S and R166S-K169E thus specifically confirming their role in recognizing Env trimer sugars when the virus escapes. The data illustrate that the CDRH2 sialic acid specific somatic mutations contribute to CAP256 bnAb binding to conserved glycans and may anchor the Abs to the virus as it tries to escape through changes in the protein sequence. Altogether, these results suggest that glycan-specific maturation of the CAP256 V2 apex bnAb lineages provides a means to counter virus escape and this in turn helps the Ab lineage to maintain a course toward bnAb development. The proposed B-cell and virus co-evolutionary pathways that lead to the generation of CAP256 and PG9 V2 apex bnAb responses are then summarized in Figure S6.

## Discussion

Understanding the molecular events of bnAb developmental pathways during natural infection can provide valuable information for HIV vaccine design (Bonsignori et al., 2017). Recent Ab-virus co-evolution studies have led to a better understanding of the complex molecular events that give rise to the CAP256 bnAb lineage recognizing the V2 apex of the Env spike (Bhiman et al., 2015; Doria-Rose et al., 2016; Doria-Rose et al., 2014). This Ab lineage was triggered by the superinfecting virus Env sequence, or a close descendant, that showed significant binding to the unmutated common ancestor (UCA) Ab. Viral envelope diversification around the strand C residues in the V2 loop was coincident with broadening of the neutralization by CAP256 Abs against diverse isolates. However, it was largely unclear how the Ab genetic determinants, either germline-encoded or acquired during affinity maturation, maintain interaction with a constantly diversifying virus, to keep the Ab lineage on a bnAb developmental pathway. Here we carried out a series of experiments to better understand the critical Ab determinants and their role in the evolution of bnAbs.

We noted earlier that CAP256.09 and PG9 V2 apex bnAb precursors possess germline-encoded motifs in their CDRH3 and CDRH2 that interact with the V2 protein and glycan core epitope allowing them to bind to some native Env trimers in their unmutated ancestor Ab configurations. This property of V2 apex bnAbs provides an opportunity to base B cell precursor-targeting priming immunogens on native-like trimer conformation rather than designed non-native structures, and thereby to potentially restrict the initial Ab angle of approach to more nativelike conformations.

Here, we observed a conserved pattern of sialic acid binding affinity maturation in the CDRH2 region of two genetically related independent Ab lineages. The somatic mutations appeared to facilitate recognition of a terminal sialic acid, possibly on the N156 glycan at the apex of the Env trimer. Phylogenetic analysis revealed the selective development of CAP256 Ab sub-lineage members that bore these glycan-specific somatic mutations. These mutations likely helped the CAP256 Ab sub-lineage members to firmly bind to the Env glycans in germinal centers to compete with the non-glycan reactive Ab sub-lineage members, thus giving them a selective advantage (Figure S6). Although, the accumulation of CDRH2 glycan-specific somatic mutations increased the likelihood of CAP256 Ab lineage members progressing to bnAbs, additional affinity maturation to accommodate or recognize the adjacent N160 glycan appeared to be important to acquire a bnAb phenotype.

Another important factor on the pathway to bnAbs appears to be virus diversification around the V2 apex core epitope (Bhiman et al., 2015). Indeed, a number of recent studies have shown that the viral diversification through escape generates a range of immunotypes that drive virus-Ab co-evolution pathways to expand Ab virus coverage (Bhiman et al., 2015; Doria-Rose et al., 2014; Liao et al., 2013; Moore et al., 2012; Wibmer et al., 2013). Presumably, only a subset of Ab sub-lineage members that tolerate the virus escape mutations can keep affinity maturing. Indeed, our results revealed that by virtue of recognizing a conserved glycan on Env through germline-encoded and early glycan-specific somatic mutations, the CAP256 Ab sub-lineage members maintain a cognate interaction with the would-be escaping virus. In other words, CAP256 and PG9 V2 apex bnAbs recognition of the Env glycans allows Ab evolution towards bnAbs as virus attempts to escape. It will be of interest to see if glycan-reactive bnAbs that target other HIV Env specificities use a similar strategy to counter virus escape.

A further point of interest is that the sialic acid-binding somatic mutations observed in the CDRH2 region occur proximal to the sialic acid-binding germline residues and the patterns described could potentially be used as signatures to track the developmental pathways of Ab lineage in a vaccine response aimed at inducing the PG9 or CAP256-like V2 apex bnAbs.

Finally, our study provides a germane example of how a human mAb longitudinally develops interaction with a pathogen-associated glycan, which endows it with the ability to better cope with escape in the protein part of the Ab epitope. It also highlights the need for immunogens to include authentic glycan compositions to maximize the chances of inducing bnAbs. The data will help in our efforts to design HIV immunogens with better precision and in optimizing immunization strategies to induce V2 apex bnAb responses.

# STAR+METHODS

## CONTACT FOR REAGENT AND RESOURCE SHARING

Further information and requests for resources and reagents should be directed to and will be fulfilled by Dennis R. Burton (burton@scripps.edu).

## EXPERIMENTAL MODEL AND SUBJECT DETAILS

**Cell lines—**Human Embryonic Kidney (HEK293T) cell line is a highly transfectable version of 293 human embryonic kidney cells that contain SV40 T-antigen. The FreeStyle™ 293-F cell line is derived from the 293 cells that are adapted to suspension culture in FreeStyle™ 293 Expression Medium. HEK293S GnTI- cells are human embryonic kidney cells that are transformed with adenovirus 5 DNA. These cells lack N-acetyl-glucosaminyltransferase I (GnTI) activity and therefore are unable to produce complex-type N-glycans. TZM-bl is a HeLa cell line that expresses CD4 receptor and CXCR4 and CCR5 chemokine co-receptors. The cell line also expresses luciferase and ß-galactosidase genes under the control of the HIV-1 promoter, hence is useful to assay in-vitro HIV infection.

## METHOD DETAILS

**Antibodies, expression and purification—**V2 apex bnAb prototypes, PG9 (PG9, PG16), CAP256.09 (CAP256.01-CAP256.32 and CAP256I1-12, CAP256 UCA) described previously were included in this study (Doria-Rose et al., 2014; Walker et al., 2009). A trimer-specific V2 apex bnAb, PGT145, and a high mannose patch glycan-dependent Ab, 2G12, reported previously were used to generate Ab affinity columns for purification of soluble trimer proteins. Antibodies specific to V3-N332 high mannose glycan, PGT128, gp120–41 interface, PGT151, and a Dengue antibody (DEN3) described elsewhere were used as control Abs for various experiments (Falkowska et al., 2014; Walker et al., 2011). For antibody production, the heavy and light chain encoding plasmids were reconstituted (1:1 ratio) in Opti-MEM (Life Technologies), and cotransfected into Human Embryonic Kidney 293 FreeStyle cells (HEK293F cells) (Invitrogen) using 293fectin (Invitrogen). The suspension cells were cultured for 4–5 days in a shaker incubator at 8% CO2, 37.0°C, and 125 rpm. The antibody containing supern atants were harvested, filtered through a 0.22 mm Steriflip units (EMD Millipore) and passed over a protein A or protein G affinity column (GE Healthcare). The bound antibody was eluted from the columns in 0.1 M citric acid, pH 3.0. Column fractions containing IgG were neutralized (2M Tris-base), pooled, and dialyzed against phosphate-buffered saline (PBS), pH 7.4. IgG purity was determined by sodium dodecyl sulfate-polyacrylamide gel electrophoresis, and the concentration was determined by measuring the relative absorbance at 280 nm.

**Site directed mutagenesis—**The amino acid point mutations in the antibody encoding plasmids and the HIV envelope plasmids were incorporated by using a QuikChange site-directed mutagenesis kit (Agilent Technologies, USA), according to the manufacturer's instructions. All the mutations were confirmed by DNA sequence analysis (Eton Bioscience, San Diego, CA).

**Pseudovirus production—**To produce pseudoviruses, Env-encoding plasmids were cotransfected with an Env-deficient backbone plasmid (pSG3ΔEnv) (1:2 ratio) using X-tremeGENE™ 9 (Sigma-Aldrich) DNA transfection reagent. Briefly, $1\times10^6$ cells in 10ml of Dulbecco's Modified Eagle Medium (DMEM) were seeded in a 100mm × 20mm cell culture dish (Corning) one day prior to transfection. For transfection, 40μl of X-tremeGENE™ 9 was added to 700μl of Opti-MEM I reduced serum medium (Thermo Fisher) in tube 1. The Env-encoding plasmid (5 μg) and pSG3ΔEnv (10 μg) were added to tube 2 in 700μl of Opti-MEM. The tube 1 and tube 2 solutions were mixed together and incubated for 25 min at room temperature. Next, the transfection mixture was added to the media with 293T cells seeded previously and then distributed uniformly. To produce glycan-modified pseudovirus variants (Glycovariants: (GVT)) of CRF250 Env, we added the α-mannosidase I and II inhibitors, kifunensine (Tocris) and swainsonine (Cayman) respectively, at a final concentration of 25 μM, to the 293T cells on the day of transfection. All pseudoviruses were harvested 48–72 h posttransfection, filtered through 0.22 mm Steriflip units (EMD Millipore) and aliquoted for use in neutralization assays.

**Neutralization assay—**Neutralization was measured by using single-round replication-defective HIV Env-pseudoviruses and TZM-bl target cells (Montefiori, 2005; Seaman et al., 2010). 25ul of 3-fold serially diluted mAbs were pre-incubated at 37°C for 1h with 25ul of tissue culture infective dose-50 (TCID50) Env-pseudotyped virus in a half-area 96-well tissue culture plate. TZM-bl target cells (5,000 cells/well) in 50μl of DMEM were added and the plates were allowed to grow in humidified incubator at 37°C and 5% Co $_2$. The luciferase activity of the lysed cells was read on instrument (Biotek) after 2–3 days, by adding lysis buffer followed by Brightglow (Promega). The 50% inhibitory concentration (IC50) was reported as the antibody concentration required to reduce infection by half.

**Recombinant envelope protein expression and purification—**Recombinant envelope proteins were expressed in HEK293F or HEK293S cells as described elsewhere (Sanders et al., 2013). Briefly, the CRF250 SOSIP.664 or BG505 SOSIP.664 encoding plasmids was cotransfected, with a plasmid encoding for Furin (3:1 ratio) specific for R6-cleavage site (RRRRRR), into HEK293F cells using PEI-MAX 4000 transfection reagent (*Polysciences, Inc.*). To produce the CRF250 SOSIP.664 trimer proteins with varying glycan composition, the glycosidase inhibitors kifunensine and swainsonine were added to the HEK293F cell cultures at a final concentration of 25 μM at the time of transfection (Doores and Burton, 2010). The CRF250 SOSIP.664 was grown in GnT1-deficient (GnT1−/−) HEK293S cells to produce a $Man_{5–9}GlcNAc_2$ glycan containing trimer. The CRF250 SOSIP.664 gp140 WT and glycovariant trimers were purified from supernatants using a 2G12 Ab antibody affinity column while BG505 trimer and CRF250 WT trimer used for other experiments were purified with a bnAb PGT145 affinity column as described previously (Pugach et al., 2015; Sanders et al., 2013). The affinity-purified proteins were size exclusion chromatography (SEC)-purified with a Superdex 200 10/300 GL column (GE Healthcare) in PBS.

**Bio Layer Interferometry (BLI) binding assay—**The binding experiments of Abs to WT and glycan modified purified trimers were performed with an Octet K2 system

(ForteBio, Pall Life Sciences). Briefly, the mAbs or IgGs (10 ug/mL in PBST) were immobilizing onto hydrated anti-human IgG-Fc biosensors (AHC: ForteBio) for 60 seconds to achieve a binding response of at least 1.0. After Ab capture, the sensor was placed in a PBST wash buffer to remove the unbound Ab to establish a baseline signal. Next, the IgG immobilized sensor was dipped into a solution containing SOSIP.664 trimer protein as analyte and incubated for 120 seconds at 1000 rpm. Following this, the trimer bound to IgG immobilized sensor was removed from the analyte solution and placed into the PBST buffer for 240 seconds at 1000 rpm. The 2 and 4 minute binding intervals respectively denote the association and dissociation binding curves reported in this study. The sensograms were corrected with the blank reference and fit (1:1 binding kinetics model) with the ForteBio Data Analysis version.9 software using the global fitting function. The data is represented as maximum binding response or the association and dissociation curve fits.

**Glycan Microarray—**Abs were assessed for glycan reactivity with amine functional glycans printed onto NHS-activated glass slides as previously described (Shivatare et al., 2016). Briefly, amine-functionalized glycans were printed in replicates of three onto NHS-activated glass slides at a concentration of 100 mM. Printed slides were allowed to react in an atmosphere of 80% humidity for 2 hour followed by desiccation overnight, and stored at room temperature in a desiccator until use. The slides were blocked with ethanolamine (50mM ethanolamine in borate buffer, pH9.2) just before use. Monoclonal antibodies (10 μg in 50μl PBS) were pre-complexed with R-Phycoerythrin-AffiniPure goat anti-human IgG, Fcγ (5 μg, Jackson Immuno Research Inc.) for 1 hr at 4°C. Thes e samples were added to the glycan array and incubated at 4°C for 6 h. Furt her, the slides were sequentially washed in PBST (0.05% Tween-20), PBS and water. Arrays were scanned on an ArrayWorx microarray reader. Image analysis was carried out with Genepix Pro 6.0 analysis software (Molecular Devices Corporation, Union City, CA) with image resolution set to 5 μm per pixel. The spots were defined as circular features with maximum diameter of 100 μm. The data was recoded as fluorescence intensity (a.u.) for all data points and is represented as average fluorescent intensity with standard deviation.

**Sialidase treatment of purified CRF250 trimer protein—**To study the role of terminal sialic acid residues in the binding of CAP256.09 and PG9 Ab prototypes, we treated PGT145 purified CRF250 trimer with sialidases or neuraminidases to linkage-specifically remove sialic acid residues following methods described previously (Lin et al., 2015; Wang et al., 2009). First, the CRF250 trimer sample was buffer exchanged to replace with the buffer system optimal for sialidase reaction. The trimer sample was treated with various sialidases from 0.5 to 8 hrs at 37°C that show different specificities for the linkage between galactose and the terminal sialic acid. These include, α2,3 sialidase from *Streptococcus pneumonia* (Sigma, N7271), which hydrolyzes non-reducing terminal α2,3-linked sialic acids from the glycans, sialidase A from *Arthrobacter ureafaciens* (Sigma, N3786) to release α2,6-linked sialic acids. The trimer sample was also treated with a mixture of four sialidases (α2,3,6,8,9) (Sigma, N7271/N3786/N2876/N8271) to remove α2,3, α2,6, α2,8, and α2,9-linked sialic acid from glycans.

**Phylogenetic analysis of CAP256 bnAbs—**Sequencing data previously obtained from donor CAP256 was downloaded from the NIH Short Read Archive and annotated with AbStar. Lineages were assigned with Clonify (Briney et al., 2016) and the CAP256 bnAb lineage was identified using homology to all CAP256 derived mAb heavy chains. All NGS sequences in the CAP256 lineage were clustered at 97.5% identity with CD-HIT (Li and Godzik, 2006), and centroid sequences for each cluster were used to construct the phylogenetic tree. A multiple sequence alignment of NGS centroid sequences, bnAb sequences (CAP256.01–32), inferred intermediates (CAP256.I1 and I2) and the CAP256 UCA was calculated with MUSCLE (Edgar, 2004); a tree file was computed with FastTree (Price et al., 2010); and the phylogenetic tree was visualized in Python using the ETE toolkit (Huerta-Cepas et al., 2010).

**Cell surface binding assay—**Binding of mAbs to the HEK293T cell-surface expressed Env trimers was performed as described previously (Walker et al., 2009). Briefly, 5-fold serial titrations of mAbs starting at 10 μg/ml were added to HEK293T cells 48-hours post-transfection with CRF250 WT and its R166 and K169 substituted Env trimer variant plasmids. The Abs were incubated with cells for 1 hr on ice on a plate rocker. The plates were washed twice in FACS buffer (1× PBS, 10% FBS) and stained with a 1:200 dilution of R-phycoerythrin (PE)-conjugated mouse antihuman IgG1 Ab (SouthernBiotech). Ab binding to surface trimers was analyzed using flow cytometry (Accuri cytometers), and the binding curves were generated by plotting the percent (%) positive cells of antigen binding as a function of antibody concentration or % positive cells as bars, at the highest Ab concentration (10 μg/ml). PGT128, a high mannose V3-N332 Ab, PGT151, a trimer dependent gp120–41 cleavage-specific Ab and DEN3, an HIV Env unrelated Ab, were used as controls to monitor the expression of well-cleaved trimers on the cell-surface.

## Supplementary Material

Refer to Web version on PubMed Central for supplementary material.

## Acknowledgments

We thank, John R. Mascola, and Nicole A. Doria-Rose for providing CAP256.08 and CAP256.09 antibodies. We thank James C. Paulson for critical comments on the manuscript and Lars Hangartner for useful discussions. This work was supported by the International AIDS Vaccine Initiative (IAVI) through Neutralizing Antibody Consortium SFP1849 (D.R.B.); the National Institute of Allergy and Infectious Diseases (Center for HIV/AIDS Vaccine Immunology and Immunogen Discovery Grant UM1AI100663) (to D.R.B.)), the Ragon Institute of MGH, MIT, and Harvard (D.R.B.). This study was made possible by the generous support of the Bill and Melinda Gates Foundation Collaboration for AIDS Vaccine Discovery (CAVD) and the American people through USAID. We thank Christina Corbaci and for her help in the preparation of figures.

## References

Amin MN, McLellan JS, Huang W, Orwenyo J, Burton DR, Koff WC, Kwong PD, Wang LX. Synthetic glycopeptides reveal the glycan specificity of HIV-neutralizing antibodies. Nature chemical biology. 2013; 9:521–526. [PubMed: 23831758]

Andrabi R, Voss JE, Liang CH, Briney B, McCoy LE, Wu CY, Wong CH, Poignard P, Burton DR. Identification of Common Features in Prototype Broadly Neutralizing Antibodies to HIV Envelope V2 Apex to Facilitate Vaccine Design. Immunity. 2015; 43:959–973. [PubMed: 26588781]

Behrens AJ, Vasiljevic S, Pritchard LK, Harvey DJ, Andev RS, Krumm SA, Struwe WB, Cupo A, Kumar A, Zitzmann N, et al. Composition and Antigenic Effects of Individual Glycan Sites of a Trimeric HIV-1 Envelope Glycoprotein. Cell reports. 2016; 14:2695–2706. [PubMed: 26972002]

Bhiman JN, Anthony C, Doria-Rose NA, Karimanzira O, Schramm CA, Khoza T, Kitchin D, Botha G, Gorman J, Garrett NJ, et al. Viral variants that initiate and drive maturation of V1V2-directed HIV-1 broadly neutralizing antibodies. Nature medicine. 2015; 21:1332–1336.

Bonsignori M, Hwang KK, Chen X, Tsao CY, Morris L, Gray E, Marshall DJ, Crump JA, Kapiga SH, Sam NE, et al. Analysis of a clonal lineage of HIV-1 envelope V2/V3 conformational epitope-specific broadly neutralizing antibodies and their inferred unmutated common ancestors. Journal of virology. 2011; 85:9998–10009. [PubMed: 21795340]

Bonsignori M, Liao HX, Gao F, Williams WB, Alam SM, Montefiori DC, Haynes BF. Antibody-virus co-evolution in HIV infection: paths for HIV vaccine development. Immunological reviews. 2017; 275:145–160. [PubMed: 28133802]

Briney B, Le K, Zhu J, Burton DR. Clonify: unseeded antibody lineage assignment from next-generation sequencing data. Sci Rep. 2016a; 6:23901. [PubMed: 27102563]

Briney B, Sok D, Jardine JG, Kulp DW, Skog P, Menis S, Jacak R, Kalyuzhniy O, de Val N, Sesterhenn F, et al. Tailored Immunogens Direct Affinity Maturation toward HIV Neutralizing Antibodies. Cell. 2016b; 166:1459–1470 e1411. [PubMed: 27610570]

Burton DR. Antibodies, viruses and vaccines. Nature reviews Immunology. 2002; 2:706–713.

Cao L, Diedrich JK, Kulp DW, Pauthner M, He L, Park SR, Sok D, Su CY, Delahunty CM, Menis S, et al. Global site-specific N-glycosylation analysis of HIV envelope glycoprotein. Nature communications. 2017; 8:14954.

Dimitrov DS. Therapeutic antibodies, vaccines and antibodyomes. MAbs. 2010; 2:347–356. [PubMed: 20400863]

Doores KJ, Burton DR. Variable loop glycan dependency of the broad and potent HIV-1-neutralizing antibodies PG9 and PG16. Journal of virology. 2010; 84:10510–10521. [PubMed: 20686044]

Doria-Rose NA, Bhiman JN, Roark RS, Schramm CA, Gorman J, Chuang GY, Pancera M, Cale EM, Ernandes MJ, Louder MK, et al. New Member of the V1V2-Directed CAP256-VRC26 Lineage That Shows Increased Breadth and Exceptional Potency. Journal of virology. 2016; 90:76–91.

Doria-Rose NA, Schramm CA, Gorman J, Moore PL, Bhiman JN, DeKosky BJ, Ernandes MJ, Georgiev IS, Kim HJ, Pancera M, et al. Developmental pathway for potent V1V2-directed HIV-neutralizing antibodies. Nature. 2014; 509:55–62. [PubMed: 24590074]

Dosenovic P, von Boehmer L, Escolano A, Jardine J, Freund NT, Gitlin AD, McGuire AT, Kulp DW, Oliveira T, Scharf L, et al. Immunization for HIV-1 Broadly Neutralizing Antibodies in Human Ig Knockin Mice. Cell. 2015; 161:1505–1515. [PubMed: 26091035]

Edgar RC. MUSCLE: multiple sequence alignment with high accuracy and high throughput. Nucleic acids research. 2004; 32:1792–1797. [PubMed: 15034147]

Escolano A, Steichen JM, Dosenovic P, Kulp DW, Golijanin J, Sok D, Freund NT, Gitlin AD, Oliveira T, Araki T, et al. Sequential Immunization Elicits Broadly Neutralizing Anti-HIV-1 Antibodies in Ig Knockin Mice. Cell. 2016; 166:1445–1458 e1412. [PubMed: 27610569]

Falkowska E, Le KM, Ramos A, Doores KJ, Lee JH, Blattner C, Ramirez A, Derking R, van Gils MJ, Liang CH, et al. Broadly neutralizing HIV antibodies define a glycan-dependent epitope on the prefusion conformation of gp41 on cleaved envelope trimers. Immunity. 2014; 40:657–668. [PubMed: 24768347]

Georgiev IS, Doria-Rose NA, Zhou T, Kwon YD, Staupe RP, Moquin S, Chuang GY, Louder MK, Schmidt SD, Altae-Tran HR, et al. Delineating antibody recognition in polyclonal sera from patterns of HIV-1 isolate neutralization. Science. 2013; 340:751–756. [PubMed: 23661761]

Gorman J, Soto C, Yang MM, Davenport TM, Guttman M, Bailer RT, Chambers M, Chuang GY, DeKosky BJ, Doria-Rose NA, et al. Structures of HIV-1 Env V1V2 with broadly neutralizing antibodies reveal commonalities that enable vaccine design. Nature structural & molecular biology. 2016; 23:81–90.

Gristick HB, von Boehmer L, West AP Jr, Schamber M, Gazumyan A, Golijanin J, Seaman MS, Fatkenheuer G, Klein F, Nussenzweig MC, et al. Natively glycosylated HIV-1 Env structure

reveals new mode for antibody recognition of the CD4-binding site. Nature structural & molecular biology. 2016; 23:906–915.

Huerta-Cepas J, Dopazo J, Gabaldon T. ETE: a python Environment for Tree Exploration. BMC Bioinformatics. 2010; 11:24. [PubMed: 20070885]

Jardine J, Julien JP, Menis S, Ota T, Kalyuzhniy O, McGuire A, Sok D, Huang PS, MacPherson S, Jones M, et al. Rational HIV immunogen design to target specific germline B cell receptors. Science. 2013; 340:711–716. [PubMed: 23539181]

Jardine JG, Ota T, Sok D, Pauthner M, Kulp DW, Kalyuzhniy O, Skog PD, Thinnes TC, Bhullar D, Briney B, et al. HIV-1 VACCINES. Priming a broadly neutralizing antibody response to HIV-1 using a germlinetargeting immunogen. Science. 2015; 349:156–161. [PubMed: 26089355]

Julien JP, Cupo A, Sok D, Stanfield RL, Lyumkis D, Deller MC, Klasse PJ, Burton DR, Sanders RW, Moore JP, et al. Crystal structure of a soluble cleaved HIV-1 envelope trimer. Science. 2013; 342:1477–1483. [PubMed: 24179159]

Landais E, Huang X, Havenar-Daughton C, Murrell B, Price MA, Wickramasinghe L, Ramos A, Bian CB, Simek M, Allen S, et al. Broadly Neutralizing Antibody Responses in a Large Longitudinal Sub-Saharan HIV Primary Infection Cohort. PLoS pathogens. 2016; 12:e1005369. [PubMed: 26766578]

Lee JH, Andrabi R, Su CY, Yasmeen A, Julien JP, Kong L, Wu NC, McBride R, Sok D, Pauthner M, et al. A Broadly Neutralizing Antibody Targets the Dynamic HIV Envelope Trimer Apex via a Long, Rigidified, and Anionic beta-Hairpin Structure. Immunity. 2017; 46:690–702. [PubMed: 28423342]

Li W, Godzik A. Cd-hit: a fast program for clustering and comparing large sets of protein or nucleotide sequences. Bioinformatics. 2006; 22:1658–1659. [PubMed: 16731699]

Liao HX, Lynch R, Zhou T, Gao F, Alam SM, Boyd SD, Fire AZ, Roskin KM, Schramm CA, Zhang Z, et al. Co-evolution of a broadly neutralizing HIV-1 antibody and founder virus. Nature. 2013; 496:469–476. [PubMed: 23552890]

Lin CW, Tsai MH, Li ST, Tsai TI, Chu KC, Liu YC, Lai MY, Wu CY, Tseng YC, Shivatare SS, et al. A common glycan structure on immunoglobulin G for enhancement of effector functions. Proceedings of the National Academy of Sciences of the United States of America. 2015; 112:10611–10616. [PubMed: 26253764]

MacLeod DT, Choi NM, Briney B, Garces F, Ver LS, Landais E, Murrell B, Wrin T, Kilembe W, Liang CH, et al. Early Antibody Lineage Diversification and Independent Limb Maturation Lead to Broad HIV-1 Neutralization Targeting the Env High-Mannose Patch. Immunity. 2016; 44:1215–1226. [PubMed: 27192579]

McGuire AT, Gray MD, Dosenovic P, Gitlin AD, Freund NT, Petersen J, Correnti C, Johnsen W, Kegel R, Stuart AB, et al. Specifically modified Env immunogens activate B-cell precursors of broadly neutralizing HIV-1 antibodies in transgenic mice. Nature communications. 2016; 7:10618.

McLellan JS, Pancera M, Carrico C, Gorman J, Julien JP, Khayat R, Louder R, Pejchal R, Sastry M, Dai K, et al. Structure of HIV-1 gp120 V1/V2 domain with broadly neutralizing antibody PG9. Nature. 2011; 480:336–343. [PubMed: 22113616]

Montefiori, DC. Evaluating neutralizing antibodies against HIV, SIV, and SHIV in luciferase reporter gene assays. In: Coligan, John E., et al., editors. Current protocols in immunology. 2005. *Chapter 12*, Unit 12.11

Moore PL, Gray ES, Wibmer CK, Bhiman JN, Nonyane M, Sheward DJ, Hermanus T, Bajimaya S, Tumba NL, Abrahams MR, et al. Evolution of an HIV glycan-dependent broadly neutralizing antibody epitope through immune escape. Nature medicine. 2012; 18:1688–1692.

Mouquet H, Scharf L, Euler Z, Liu Y, Eden C, Scheid JF, Halper-Stromberg A, Gnanapragasam PN, Spencer DI, Seaman MS, et al. Complex-type N-glycan recognition by potent broadly neutralizing HIV antibodies. Proceedings of the National Academy of Sciences of the United States of America. 2012; 109:E3268–3277. [PubMed: 23115339]

Pancera M, Shahzad-Ul-Hussan S, Doria-Rose NA, McLellan JS, Bailer RT, Dai K, Loesgen S, Louder MK, Staupe RP, Yang Y, et al. Structural basis for diverse N-glycan recognition by HIV-1-neutralizing V1–V2-directed antibody PG16. Nature structural & molecular biology. 2013; 20:804–813.

Panico M, Bouche L, Binet D, O'Connor MJ, Rahman D, Pang PC, Canis K, North SJ, Desrosiers RC, Chertova E, et al. Mapping the complete glycoproteome of virion-derived HIV-1 gp120 provides insights into broadly neutralizing antibody binding. Sci Rep. 2016; 6:32956. [PubMed: 27604319]

Price MN, Dehal PS, Arkin AP. FastTree 2–approximately maximum-likelihood trees for large alignments. PloS one. 2010; 5:e9490. [PubMed: 20224823]

Pugach P, Ozorowski G, Cupo A, Ringe R, Yasmeen A, de Val N, Derking R, Kim HJ, Korzun J, Golabek M, et al. A native-like SOSIP.664 trimer based on a HIV-1 subtype B env gene. Journal of virology. 2015

Rappuoli R, Bottomley MJ, D'Oro U, Finco O, De Gregorio E. Reverse vaccinology 2.0: Human immunology instructs vaccine antigen design. The Journal of experimental medicine. 2016; 213:469–481. [PubMed: 27022144]

Sanders RW, Derking R, Cupo A, Julien JP, Yasmeen A, de Val N, Kim HJ, Blattner C, de la Pena AT, Korzun J, et al. A next-generation cleaved, soluble HIV-1 Env trimer, BG505 SOSIP.664 gp140, expresses multiple epitopes for broadly neutralizing but not non-neutralizing antibodies. PLoS pathogens. 2013; 9:e1003618. [PubMed: 24068931]

Sanders RW, van Gils MJ, Derking R, Sok D, Ketas TJ, Burger JA, Ozorowski G, Cupo A, Simonich C, Goo L, et al. HIV-1 VACCINES. HIV-1 neutralizing antibodies induced by native-like envelope trimers. Science. 2015; 349:aac4223. [PubMed: 26089353]

Seaman MS, Janes H, Hawkins N, Grandpre LE, Devoy C, Giri A, Coffey RT, Harris L, Wood B, Daniels MG, et al. Tiered categorization of a diverse panel of HIV-1 Env pseudoviruses for assessment of neutralizing antibodies. Journal of virology. 2010; 84:1439–1452. [PubMed: 19939925]

Shivatare SS, Chang SH, Tsai TI, Tseng SY, Shivatare VS, Lin YS, Cheng YY, Ren CT, Lee CC, Pawar S, et al. Modular synthesis of N-glycans and arrays for the hetero-ligand binding analysis of HIV antibodies. Nat Chem. 2016; 8:338–346. [PubMed: 27001729]

Sok D, van Gils MJ, Pauthner M, Julien JP, Saye-Francisco KL, Hsueh J, Briney B, Lee JH, Le KM, Lee PS, et al. Recombinant HIV envelope trimer selects for quaternary-dependent antibodies targeting the trimer apex. Proceedings of the National Academy of Sciences of the United States of America. 2014; 111:17624–17629. [PubMed: 25422458]

Steichen JM, Kulp DW, Tokatlian T, Escolano A, Dosenovic P, Stanfield RL, McCoy LE, Ozorowski G, Hu X, Kalyuzhniy O, et al. HIV Vaccine Design to Target Germline Precursors of Glycan-Dependent Broadly Neutralizing Antibodies. Immunity. 2016; 45:483–496. [PubMed: 27617678]

Tian M, Cheng C, Chen X, Duan H, Cheng HL, Dao M, Sheng Z, Kimble M, Wang L, Lin S, et al. Induction of HIV Neutralizing Antibody Lineages in Mice with Diverse Precursor Repertoires. Cell. 2016; 166:1471–1484 e1418. [PubMed: 27610571]

Walker LM, Huber M, Doores KJ, Falkowska E, Pejchal R, Julien JP, Wang SK, Ramos A, Chan-Hui PY, Moyle M, et al. Broad neutralization coverage of HIV by multiple highly potent antibodies. Nature. 2011; 477:466–470. [PubMed: 21849977]

Walker LM, Phogat SK, Chan-Hui PY, Wagner D, Phung P, Goss JL, Wrin T, Simek MD, Fling S, Mitcham JL, et al. Broad and potent neutralizing antibodies from an African donor reveal a new HIV-1 vaccine target. Science. 2009; 326:285–289. [PubMed: 19729618]

Walker LM, Simek MD, Priddy F, Gach JS, Wagner D, Zwick MB, Phogat SK, Poignard P, Burton DR. A limited number of antibody specificities mediate broad and potent serum neutralization in selected HIV-1 infected individuals. PLoS pathogens. 2010; 6:e1001028. [PubMed: 20700449]

Wang CC, Chen JR, Tseng YC, Hsu CH, Hung YF, Chen SW, Chen CM, Khoo KH, Cheng TJ, Cheng YS, et al. Glycans on influenza hemagglutinin affect receptor binding and immune response. Proceedings of the National Academy of Sciences of the United States of America. 2009; 106:18137–18142. [PubMed: 19822741]

Wibmer CK, Bhiman JN, Gray ES, Tumba N, Abdool Karim SS, Williamson C, Morris L, Moore PL. Viral escape from HIV-1 neutralizing antibodies drives increased plasma neutralization breadth through sequential recognition of multiple epitopes and immunotypes. PLoS pathogens. 2013; 9:e1003738. [PubMed: 24204277]

Xiao X, Chen W, Feng Y, Zhu Z, Prabakaran P, Wang Y, Zhang MY, Longo NS, Dimitrov DS. Germline-like predecessors of broadly neutralizing antibodies lack measurable binding to HIV-1

envelope glycoproteins: implications for evasion of immune responses and design of vaccine immunogens. Biochemical and biophysical research communications. 2009; 390:404–409. [PubMed: 19748484]

## Highlights

- CAP256 V2 apex bnAbs affinity mature with sialic acid (SIA)-bearing HIV Env glycans
- Both germline and somatic-mutated HC-Ab residues contribute to SIA recognition
- SIA-specific maturation pattern is conserved in two genetically-related bnAb lineages
- SIA-specific affinity maturation counters virus escape and helps bnAb development

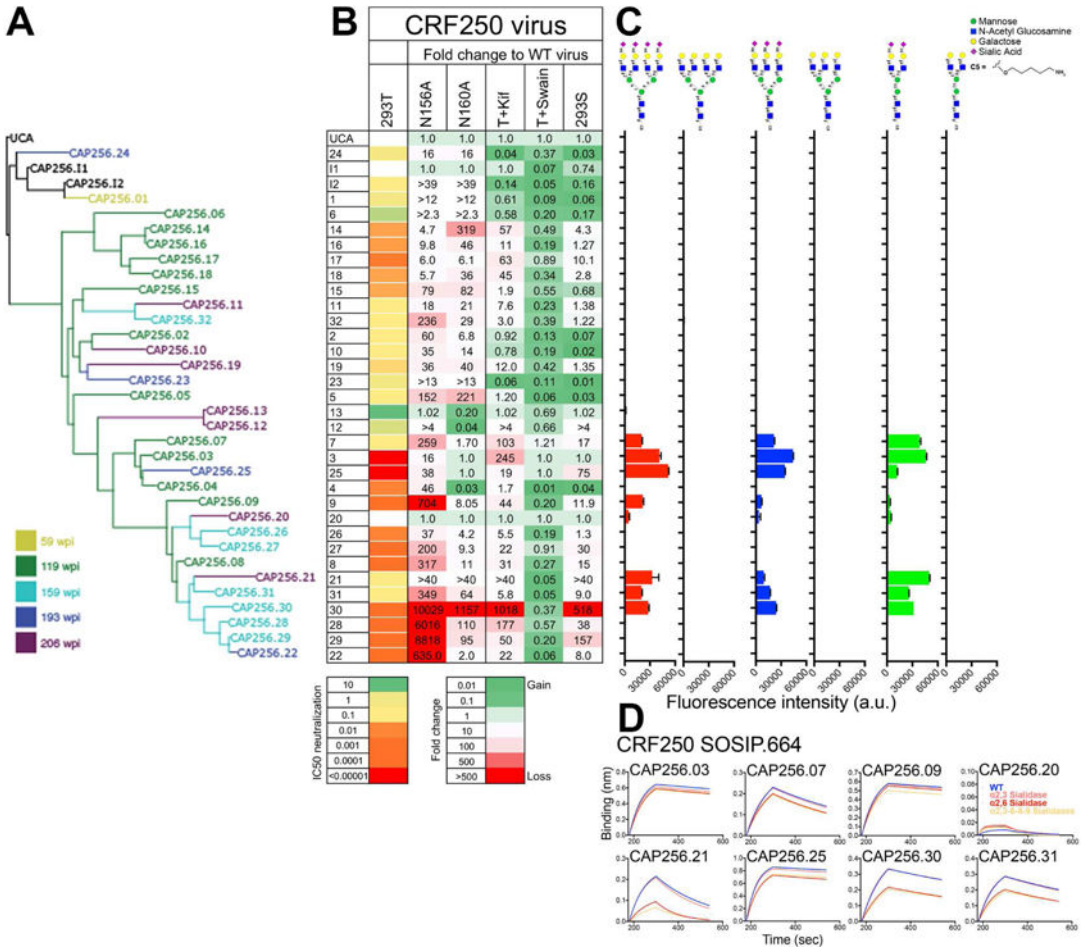


**Figure 1. CAP256 lineage Abs show varying glycan specificity and sialic acid reactivity as measured by neutralization, glycan array and Env trimer binding**

**A**. A phylogenetic tree based on the variable heavy (VH) chain region of CAP256 lineage monoclonal antibodies (CAP256.01-32, I1 and I2). The tree originates from the VH3-30*18 germline gene present in CAP256 UCA. The Abs are colored based on time of sampling (wpi: weeks post infection) **B**. Heatmap representation of the IC50 neutralization titers of the CAP256 Abs with CRF250 wild-type virus (293T). Fold changes in the IC50 neutralization titers of the CAP256 bnAbs for CRF250 glycan eliminated variants at positions N156 (N156A) and N160 (N160A) and viral glycovariants produced in presence of glycosidase inhibitors (kifunensine (Kif) and swainsonine (Swain)) or in a 293S cell line, which lacks an N-acetyl glucosaminyl transferase enzyme. The mAbs were tested in a TZM-bl cell based infectivity assay (Ab concentration range (IC50 < 0.00001 or >10 μg/ml) and the neutralization IC50 fold changes are represented in heatmap format as indicated in the key. An IC50 fold change value of 1.0 indicates that IC50 neutralization titer is unchanged between the WT virus (293T) and the virus variant. **C**. Reactivity of the CAP256 Abs to glycans on glycan microarrays. Binding is represented as fluorescence intensity (a.u.). The symbols for each monosaccharide are indicated. **D**. Octet binding response of the CAP256 bnAbs to CRF250 WT trimer and its three desialylated forms (α2,3 or α2,6 alone or α2,3,6,8,9 cocktail sialidase-treated trimers). The mAbs were immobilized onto an anti-

human IgG-Fc sensor followed by dipping these biosensors into the trimer solution and the Ab-trimer interaction is represented as binding curves showing the association (120 seconds; 180–300) and dissociation (240 seconds; 300–540). See also Figure S1 and S2

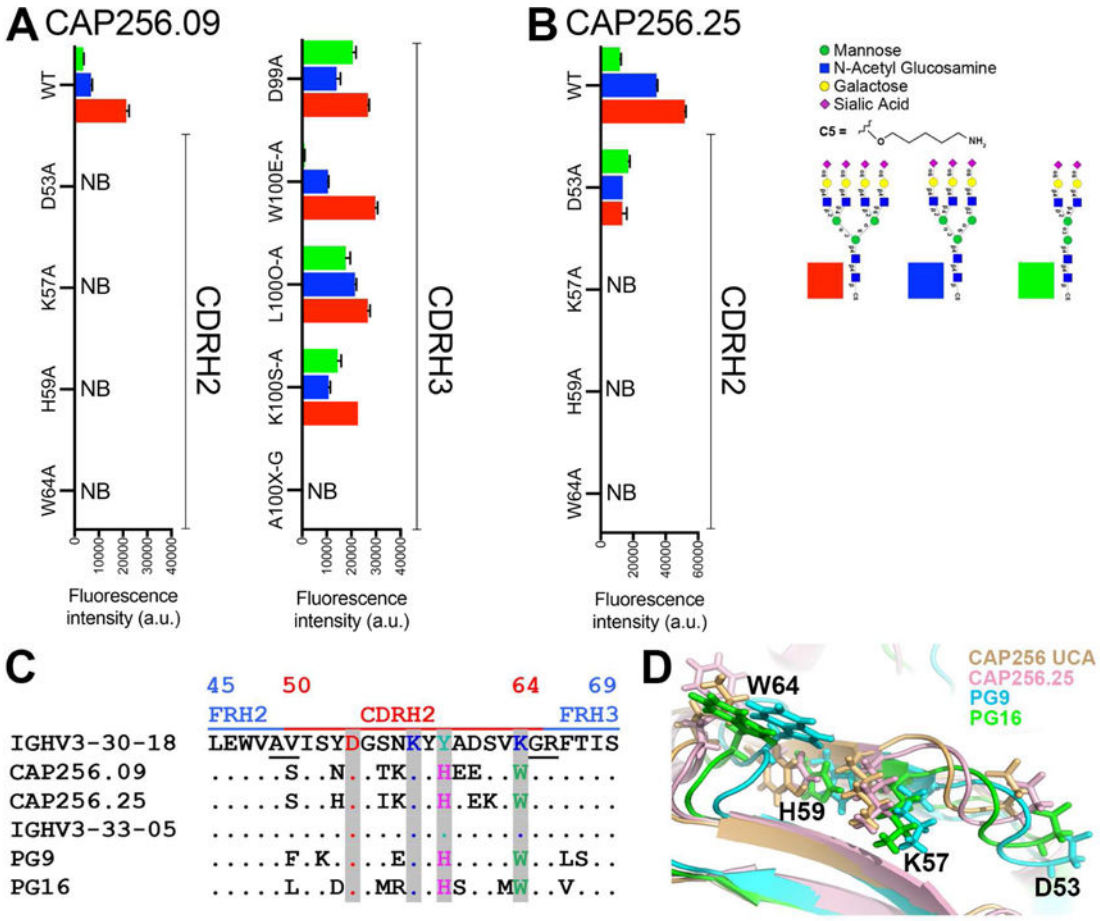


**Figure 2. CDRH2 germline encoded and somatically mutated residues of CAP256.09 and CAP256.25 Abs are important in sialic acid recognition on glycan arrays**

**A**. Reactivity on glycan microarrays of CAP256.09 wild type (WT) antibody and 9 variants. The 9 amino acid substitutions in the CAP256.09 heavy chain variable region include 4 in CDRH2 and 5 in CDRH3. **B**. Binding of CAP256.25 WT, CDRH2 Ab variants to glycan on the glycan microarray. **C**. Amino acid sequence alignment of the CDRH2 and parts of the FRH2 and FRH3 region of CAP256.09 and PG9 V2 apex bnAb prototypes with their respective germline VH-genes. Kabat numbering is indicated. The alignment shows that both V2 apex bnAb prototypes retain the germline-encoded residues at CDRH2 positions D53 and K57 and accumulate two common somatic mutations (Y59H and K64W). **D**. Structural alignment of CAP256 UCA (wheat), CAP256.25 (light pink), PG9 (cyan) and PG16 (green) bnAbs highlighting 4 amino acid positions in the CDRH2 region with side chains as sticks. See also Figure S3

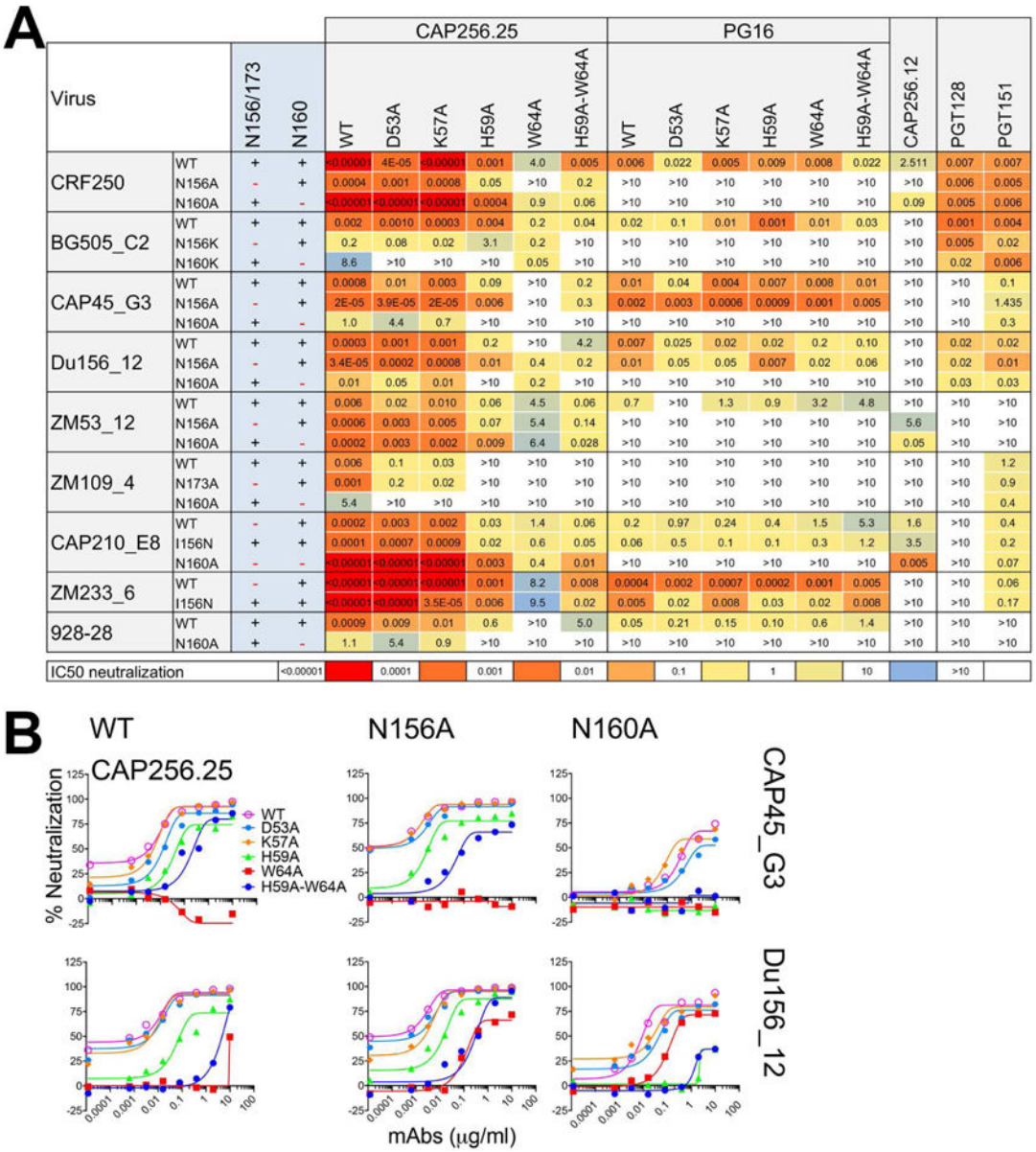


**Figure 3. Neutralization of a panel of viruses and glycovariant viruses suggests that CAP256.25 Ab CDRH2 residues interact with sialic acid likely on N156 glycan**

**A**. Neutralization of a panel of viruses including N156 or 173A and N160A variants by CAP256.25 and PG16 Abs and their CDRH2 variants. Neutralization heat maps based on the IC50 titers show the effect of glycan removals on antibody neutralizing activity. PGT128, an N332-V3 Ab and PGT151, a gp120-41 interface Ab, were used as controls. **B**. Neutralization titration of CAP256.25 WT Ab and its CDRH2 substituted variants against two representative viruses, CAP45_G3 and Du156.12 and their glycan eliminated N156A, N160A variants.

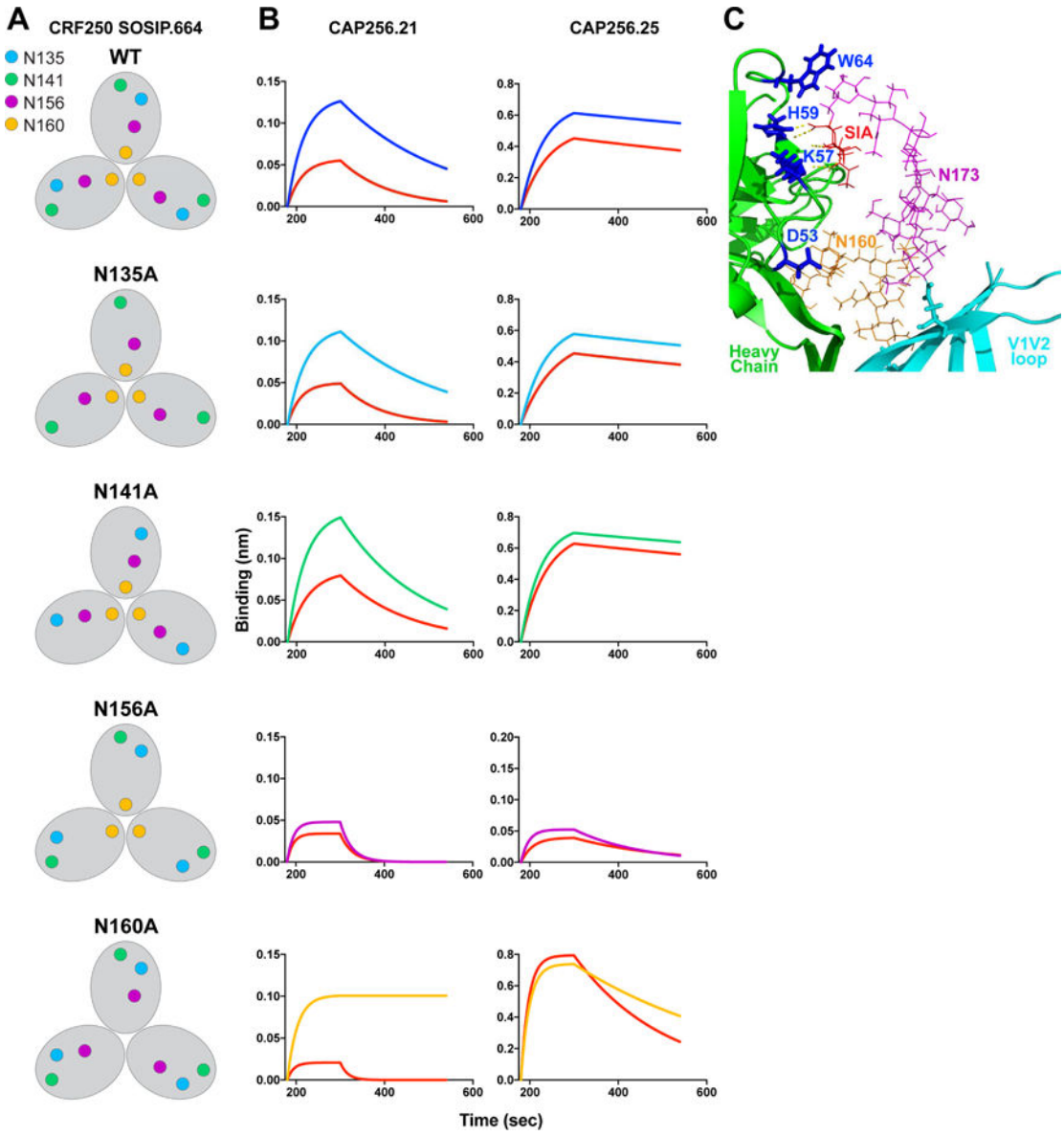


**Figure 4. Binding of select CAP256 Abs to CRF250 trimer V2 apex glycan variants shows varying sensitivity to α2,6 sialidase treatment**

**A**. Schematic representation of the V2 apex individual glycan substituted variants on CRF250 SOSIP.664 trimer backbone. **B**. Octet binding curves (association: 120 s; (180–300) and dissociation: 240 s; (300–540)) of CAP256.21 and CAP256.25 Abs with CRF250 trimer glycovariants. The binding response of CAP256.25 bnAb with the CRF250 N156A variant is fixed to 0.2 nanometer (nm) for clarity **C**. Ribbon representation of PG16 antibody (green) in complex with isolate ZM109F V1V2 loop (cyan) on a scaffold (modified from (Pancera et al., 2013)). The glycans at N160 (orange; shown as lines) and N173 (magenta; shown as lines) positions and the sialic acid residue (SIA; red) are labeled. The PG16 heavy chain CDRH2 residues (D53, K57, H59 and W64) are highlighted (blue). The residues K57 and H59 of the PG16 heavy chain show hydrogen bonding (yellow dotted line) with a terminal sialic acid residue of N173 glycan. See also Figure S4

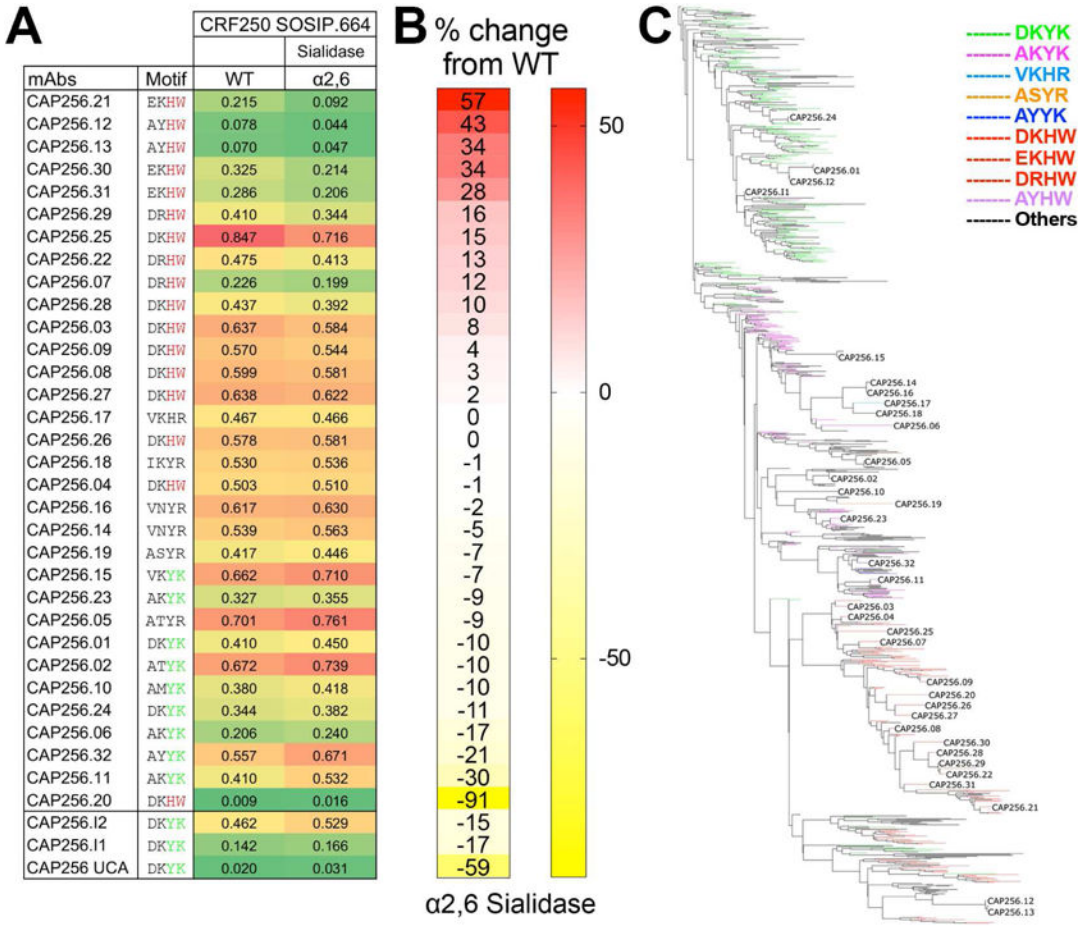


**Figure 5. Binding of the full range of CAP256 lineage Abs to CRF250 SOSIP.664 shows a gradation of sensitivity to α2,6 sialidase treatment dependent upon key HCDR2 residues**

**A**. Octet binding of CAP256-derived mAbs to PGT145 Ab-affinity purified CRF250 SOSIP.664 trimer (WT) and α2,6 desialylated version. The CAP256 mAbs were captured on an anti-human IgG-Fc sensor and then the CRF250 trimer forms (100nM) flowed over. The binding response (nanometers (nm)) to WT and the α2,6 desialylated trimers is shown as color-coded numerical values and the CAP256 mAbs are arranged with respect to their binding sensitivity to α2,6 desialylated CRF250 trimer. The four amino acids position in the CDRH2 (with respect to germline positions D53, K57, Y59 and K64) are indicated for each Ab. **B**. Percent (%) change in the octet binding responses are shown as heatmap for the desialylated trimer form and is calculated as (Ab binding response to the α2,6 desialylated CRF250 trimer/binding response to the CRF250 WT trimer). **C**. Phylogenetic tree showing the development of the CAP256 bnAb lineage from the VH3-30*18 germline gene. The branches in the tree are color-coded and demonstrate the evolution of amino acid residues at the above-mentioned four positions in CDRH2. The germline residues, DKYK and the most evolved residues DKHW in glycan-reactive Abs are indicated in green and red respectively. See also Figure S2C

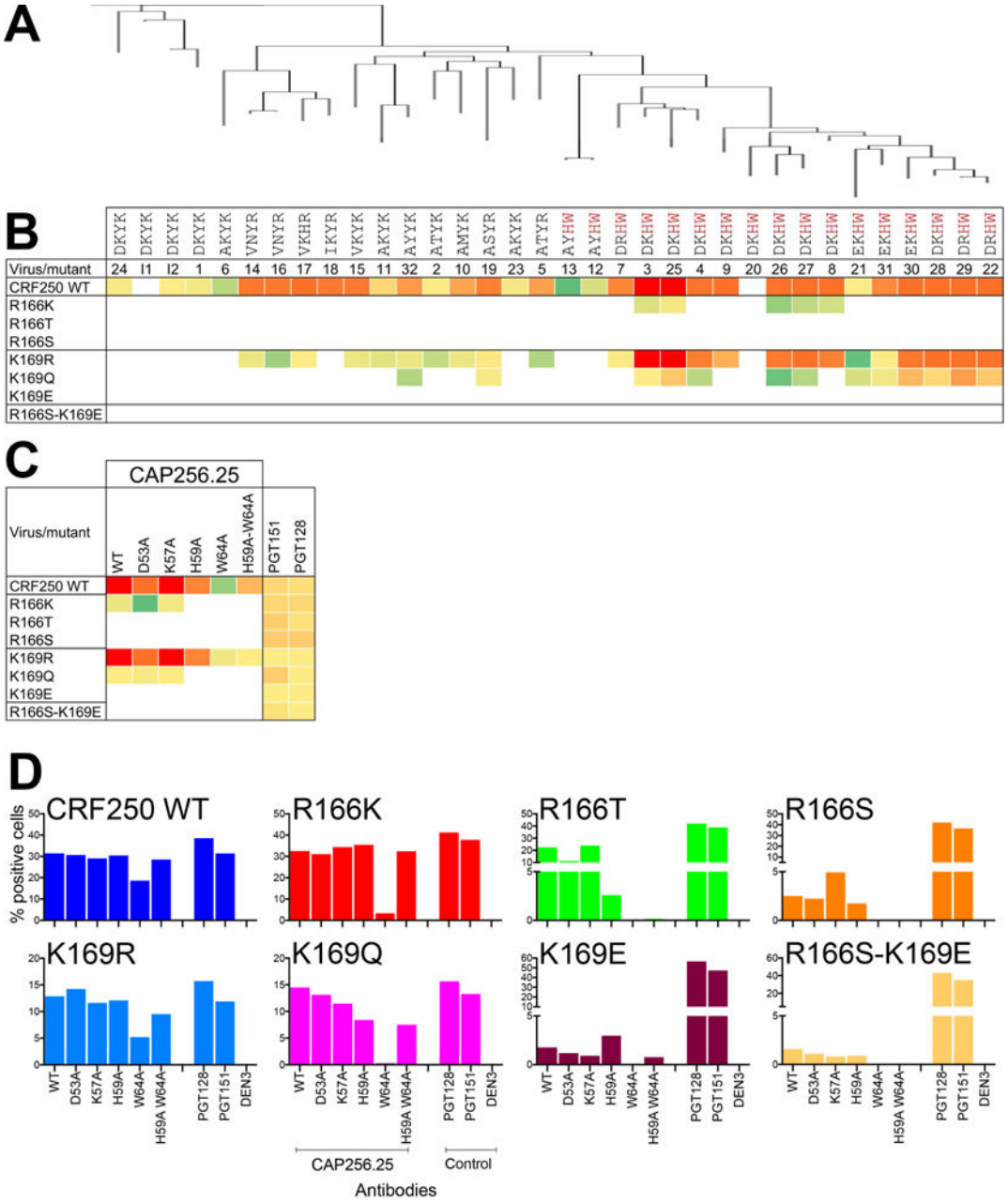


**Figure 6. Sialic acid-binding residues on CAP256.25 bnAb are critical in resisting virus escape via mutations in the basic residue-rich region of V2**

**A**. Phylogenetic tree constructed from VH sequences displaying members of the CAP256 bnAb lineage evolved from the VH3-30*18 germline gene. **B**. Neutralization heatmap based on the IC50 neutralization titers of CAP256 Ab lineage members with CRF250 WT virus and its 166 and 169 position (HXB2 numbering)-substituted variants that represent escape mutations of CAP256 Abs in natural infection (Bhiman et al., 2015). The 4 CDRH2 amino acid positions, important for glycan recognition, are shown for each Ab member. The lineage members that possess an H and W amino acid residues at positions 59 and 64 respectively are highlighted in red. **C**. Neutralization heatmap of CAP256.25 Ab and its

CDRH2 variants against CRF250 WT virus and positions 166 and 169-substituted variant viruses. **D**. Binding of CAP256.25 WT Ab and variants to 293T cell-surface expressed CRF250 WT Env and putative escape variant Env trimers. The Abs were used at a final concentration of 10 μg/ml and the extent of binding to the surface trimers is represented as % positive cells as detected by PE-conjugated anti-human-Fc secondary Ab. The V3-N332 high mannose glycan specific Ab PGT128, the gp120–41 trimer cleavage specific Ab PGT151 and a non-HIV Env epitope specific Ab DEN3 were controls for the assay. See also Figure S5 and S6